Nigerian Journal of Engineering
Faculty of Engineering
Ahmadu Bello University
Samaru - Zaria, Nigeria

Vol. 26, No. 3, December 2019
ISSN: 0794 - 4756

MODELING OF MARTENSITIC PHASE TRANSFORMATION IN MATERIAL SCIENCE: A NUMERICAL STUDY

A. A. Abubakar[1,2], N. A. Muhammad[1], D. Sh. Ibrahim[3] and D. U. Lawal[1,2]

[1]Department of Mechanical Engineering, Bayaro University, Kano
[2]Department of Mechanical Engineering, King Fahd University of Petroleum and Minerals, 31261 Dhahram KSA
[3]Department of Mechatronics Engineering, Bayaro University, Kano
Corresponding Author's Email: abbamec@yahoo.com

ABSTRACT
Phase transformation involves the formation of new phases or constituents through re-arrangement of atoms in a material microstructure. It often results in the production of new precipitates that may enhance/degrade the overall physical and mechanical properties of the parent material. In the present study, the non-linear martensitic phase transformation (or Allen-Cahn) equation was analyzed numerically using both Galerkin's Finite Element Method (FEM) and Fourier Spectral Method (FSM). Material properties corresponding to zirconia ceramic was selected for the analysis. The results from both the FEM and FSM were critically analyzed and compared in terms of computational intensity, efficiency and accuracy. The dependence of the computation on grid size and time step was also studied. The results show that it is more effective to model phase transformation using FSM.
Keywords: *Computational material science, phase transformation, materials engineering, Fourier spectral method, finite element method, phase field model.*

INTRODUCTION

Materials science/engineering is a broad scientific field that deals with the study of the correlation between the structure, properties and processing of materials. Through material science, researchers are able to identify suitable material processing methods which can result in unique structures (or arrangement of atoms) and desirable properties. Consequently, a wide variety of modern materials which can be used to produce modern day products are designed. For several centuries, material science has led the foundation for technological advancement and progress of humanity. It started right from the stone and iron age where man was able to process natural rocks and minerals into products for daily use. Today, we have gone beyond the nanoscale, where man can produce certain miniature materials having unique properties through which special products with astonishing performance can be manufactured. Due to advancement in computer technology, materials science is rapidly progressing through modeling and computation. As opposed to conventional scientific methodology, the first step of material design often involves using powerful computers which have very fast and efficient computational capabilities to simulate the structure-property-processing relationship before the experimental fabrication and testing of such materials. Consequently, a substantive amount of time, energy and resources is saved. Phase transformation (or separation) studies is among the fundamental topics of material science where computational modeling is essential in relating the material properties with microstructure evolution (Chen, 2002; Moelans *et al*., 2008).

Computational modeling of phase transformation was previously carried out using the sharp-interface model. The method is strictly applicable to very simple multi-phase system due to high computational intensity resulting from numerical solution of sets of interfacial boundary conditions at the sharp interface. Variety of sharp interface models for phase transformation in alloys can be found in DICTRA (Moelans *et al*., 2008), (Kobayashi, 1993). A more recent approach, which defines the interface as a 2D object of finite thickness is called the diffuse-interface model (Moelans, 2006). With this method, the numerical difficulty associated with the sharp-interface model is avoided as phase-field variables are used to represent interface zones with the evolving microstructure. The most popular diffuse-interface models are (Raabe, 1998): Cellular Automata, Level Set Method and the Phase Field Method.

The phase field method (PFM) is the most recent and fully-developed diffuse-interface method of simulating phase transformations. It uses a set of phase field variables (with smoothly varying interfacial properties) in tracking the evolution of the coexisting phases. The method can accurately predict the complete thermodynamics and kinetics of phase transformations in materials (Moelans *et al*., 2008). PFM has wide applications such as microstructure evolution, solidification dynamics, viscous fingering and vesicle dynamics, fracture/crack dynamics, dislocation dynamics, etc. Phase field equations are derived from thermodynamic principles through minimization of the free energy functional. The popular ones are sets of partial differential equations (PDEs) developed by Cahn and Hilliard (Cahn and Hilliard, 1958) and Allen and Cahn (Allen and Cahn, 1979) theorems for diffusional and martensitic material transformations respectively. The numerical solution of the PDEs gives the evolution of the coexisting phases in terms of space and time at less computational cost. It is more powerful than other diffuse-interface methods, since various energy contributions (such as chemical, elastic, electrostatic and magnetostatics energies) can be naturally integrated into the model.

Recently, popular numerical methods such as finite difference method (FDM), finite element method (FEM), and Fourier spectral method (FSM) have been used to solve the phase field equations. Voyiadjis and Mozaffari (Voyiadjis and Mozaffari, 2013) solved the phase field equations for non-local damage in linear elastic isotropic material using both explicit and implicit finite element schemes. They showed that the highly non-linear phase field equations are best solved by Crank Nicholson or other implicit schemes. Furihata and Matsuo (Furihata and Matsuo, 2003) developed a highly stable, convergent and conservation finite difference scheme for the numerical solution of Cahn-Hilliard equation. Benjamin *et al*. (Vollmayr-Lee and Rutenberg, 2003) also developed an unconditionally-stable and efficient finite difference scheme for numerical solution of phase field equations as applied to coarsening simulation. In the literature, very few recent works can be found on the use of FDM to solve the phase field equations. Apart from high computational costs, it is often difficult to solve realistic phase transformation problems with FDM due to numerical difficulties associated with the high non-linearity, instability and complicated periodic boundary conditions of phase field equations. Consequently, FEM is used more recently to solve the phase field equations. In this regards, Danilov and Nestler (Danilov and Nestler, 2005) used an adaptive finite element scheme to simulate growth of dendrites in binary and ternary eutectic alloys. Zaeem *et al*. (Zaeem, 2010) developed mixed-order finite element scheme for numerical solution of solid-state phase transformation in thin films subjected to diffusion couple. Abubakar *et al*. (Abubakar *et al*., 2015) used a second-order finite element scheme for numerical modeling of V_2O_5 hot corrosion in thermal barrier coatings using the phase field equations. Many other research works related to numerical solution of phase field equation with the FEM can be found in literature. The stability, convergence and implementation difficulties encountered with FDM are handled well by FEM. One unique advantage of the FEM is that, it can easily be used to define boundary condition on any boundary bounding highly complex computational domain. However, computation often becomes too intensive for problem involving 3D phase transformation. Consequently, FSM is used in many recent works to solve the phase field equations. The advantage of FSM is that, periodic boundary conditions come naturally with the method. Also, it results in least computational cost and high accuracy since computation is done in Fourier space. The only shortcoming of the method is that, it is not very stable especially when solved in irregularly-shaped domains. Due to its high computational efficiency, many recent works have focused on improving the stability of spectral methods. For instance, Vidyasagar *et al*. (2017) recently used fourier spectral scheme with improvement in stability (based on finite difference approximations) to model electro-mechanically coupled phase transformation in ferroelectric ceramics. Also, Lee *et al*. (2017) developed a more computationally efficient and highly accurate operator splitting Fourier spectral scheme for numerical modeling of phase transformation in epitaxial thin film. Similarly, Li *et al*. (2017) developed a unconditionally-stable semi-implicit Fourier spectral scheme for numerical solution of Cahn-Hilliard equation. It can be seen that, FEM and FSM have been extensively used to model phase field (transformation) equations. However, quantitative analysis of computational efficiency and resources associated with both schemes is lacking.

In the present study, the non-linear martensitic phase separation equation (developed based on Allen-Cahn theory) is analyzed numerically using Galerkin's Finite Element Method (FEM) and Fourier Spectral Method (FSM). Material properties corresponding to a famous ceramic material (zirconia) is used for the analysis. The results from both the FEM and FSM are critically analyzed and compared. The dependence of the computation on grid size and time step is also studied.

METHODOLOGY

The Allen-Cahn Equation

The Allen-Cahn equation is the time-dependent form of the Ginzburg-Laudau equation, **i**.e. non-linear reaction-diffusion PDE. It is a 2nd order PDE that describes the linear dependence of the evolution rate of the non-conserved field variable (commonly known as order parameter) on the driving force. The order parameters are used to track the spatial and temporal evolution of various phases within a given microstructure (Moelans *et al*., 2008). Order parameter (η_1) have values that range from -1 to 1. Regions having values 1 and -1 signifies a specific sub-lattice/phase, while 0 signifies unstable or disordered phase. Any value that falls between -1 to 0 and 0 to 1 signifies an interface.

Usually, the driving force for phase separation comes from the total free energy ($F(\eta_1)$) of the thermodynamic system. Phase transformation is only possible if transition occurs in such a way that the total free energy of the system decreases. In other words, phase transition occurs when a system tries to attain equilibrium by changing from state of high chemical potential (or higher free energy) to state of low chemical potential (or lower free energy). The total free energy ($F(\eta_1)$) of the system is represented as a function of phase field variables and their corresponding gradients as expressed in Equation (1) (Moelans *et al*., 2008).

$$F(\eta_1) = F_{bulk} + F_{int.} = \int (f(\eta_1) + \frac{\alpha_1}{2}^2 \cdot (\nabla \eta_1)^2) dx \cdot dy \qquad (1)$$

where,

F_{bulk} is the bulk or local free energy of the system

$F_{int.}$ is the Interfacial energy

$f(\eta_1) = \eta_1 \cdot (\eta_1 - 1) \cdot (\eta_1 + 1)$ is the free energy density represented by the usual double-well potential for a two-phase system.

α_1 is the gradient energy coefficient.

$$\frac{\partial \eta_1(x,y,t)}{\partial t} = -L_1 \cdot \frac{\delta F(\eta_1)}{\delta \eta_1} = -L_1 \left(\frac{\partial f}{\partial \eta_1} - \alpha_1 \nabla^2 \eta_1 \right) \qquad (2)$$

where, the kinetic mobility (L_1) and the gradient energy coefficients (α_1) may be constants or functions of the phase field variables (Wen *et al*., 2012).

After simplification, the Allen-Cahn equation becomes,

$$\frac{\partial \eta_1(x,y,t)}{\partial t} = -L_1(\eta_1^3 - \eta_1 - \alpha_1 \nabla^2 \eta_1) \qquad (3)$$

As the length scale for simulation is far smaller than the time scale, it is necessary to normalize Equation (3) to minimize numerical errors during computations. Assuming the normalization constants for time to be T and for spatial variables to be C, the Allen-Cahn equation reduces to:

$$\frac{\partial \eta_1(\bar{x},\bar{y},\bar{t})}{\partial \bar{t}} = \eta_1 - \eta_1^{\,3} + \varepsilon \bar{\nabla}^2 \eta_1^{\,2} \qquad (4)$$

where,

$$\bar{t} = \frac{t}{T},\ \bar{x} = \frac{x}{C},\ \bar{y} = \frac{y}{C},\ \bar{\nabla}^2\eta_1 = \frac{\bar{\nabla}^2\eta_1}{C^2},\ \varepsilon = \frac{\alpha_1}{C^2}$$

Note that the dependent variable (η_1) does not need normalization, because it actual values range from -1 to 1.

Geometry, Material Properties, Initial and Boundary Conditions

The Allen-Cahn equation will be analyzed on a 200 μm x 200 μm microstructural RVE for phase separation in zirconia ceramic with material properties, $L_1 = 2\ m^3/Js$ and $\alpha_1 = 1\times10^{-8}\ J/m$ as obtained from the works of (Abubakar *et al*., 2015).

To represent the common thermal fluctuations associated with phase transformation, the numerical analysis conducted here is tested with both simple mathematical equation and Langevin noise as demonstrated in demonstrated in Figure 1 (a). The mathematical expression used is expressed as:

$$\eta_1(\bar{x},\bar{y},0) = \frac{1}{2}(\sin 2\pi\bar{x} + 0.001\cos 16\pi\bar{x}) + \frac{1}{2}(\sin 2\pi\bar{y} + 0.001\cos 16\pi\bar{y}) \qquad (5)$$

As commonly used, the Neumann (or natural) boundary condition is applied at the outer boundaries of computational domain as expressed in Equation (6).

$$\boldsymbol{n}\cdot\nabla\boldsymbol{\eta_1} = \mathbf{0} \qquad (6)$$

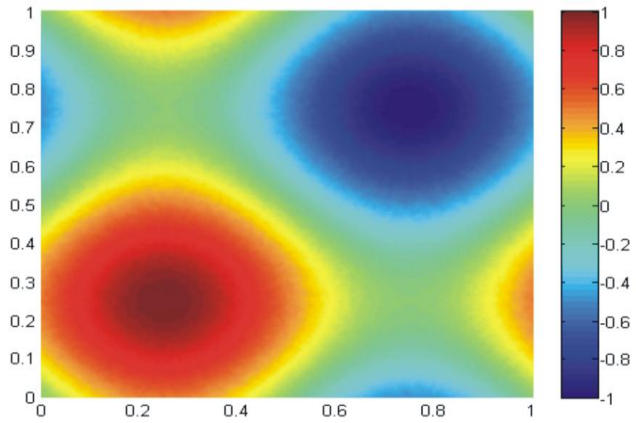

Figure 1 (a): Initial condition based on mathematical expression

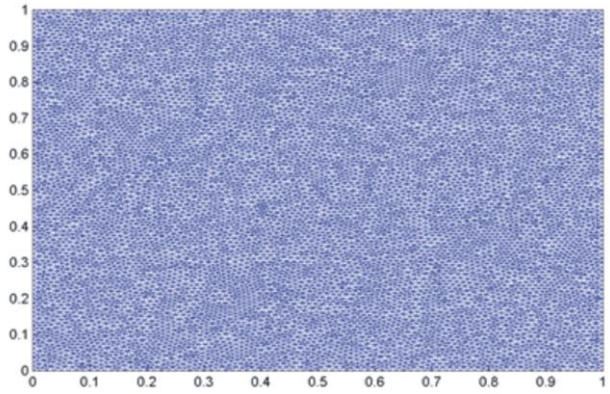

Figure 1 (b): Initial condition represented with Langevin noise

The Galerkin finite element formulation

Using mathematical procedures based on Galerkin, the PDEs are first expressed in their variational (or weak) form after which an approximate solution for the domain is sought using a space of continuous piecewise interpolation functions. The weak form PDE is obtained by multiplying the left and right-hand sides of the PDE by the basis function, φ, as expressed in Equation (7).

$$(\dot{\eta}_1,\varphi) + \varepsilon\cdot a(\eta_1,\varphi) = (f(\eta_1),\varphi) \quad ; \quad \forall\varphi\in H^1(\Omega) \qquad (7)$$

where,

$$H^1(\Omega) = \{\varphi : \varphi,\varphi' \in L_2(\Omega)\}$$

$$(\dot{\boldsymbol{\eta}}_1,\boldsymbol{\varphi}) = \int_{\boldsymbol{\Omega}} \dot{\boldsymbol{\eta}}_1\cdot\boldsymbol{\varphi}$$

$$a(\eta_1,\varphi) = \int_{\Omega}\nabla\eta_1\cdot\nabla\varphi$$

$$(f(\eta_1),\varphi) = \int_{\Omega}(\eta_1-\eta_1^{\,3})\cdot\varphi$$

The dependent variable in Equation xx is discretized by assuming the solution to be approximated with hat basis functions and certain number of finite elements as expressed Equation (8).

$$\eta_{1h} = \sum_{j=1}^{M}\xi_j(t)\Phi_j \qquad (8)$$

where, $j = 1,2,.....$, Φ_j is the hat basis function and M in the total number of nodes in mesh.

Equation (9) is discretized into system of ordinary differential equations (ODE) by adopting the approximation given in Equation (10) and taking $i, j = 1,2,.....,M$. Thus, the final discrete form is given as:

$$\sum_{j=1}^{M}\dot{\xi}_j(t)(\Phi_j,\Phi_i) + \varepsilon\cdot\sum_{j=1}^{M}\xi_j(t)(\nabla\Phi_j,\nabla\Phi_i) = (f(\xi),\Phi_i) \qquad (10)$$

In matrix form, Equation (11) can be represented as:

$$\boldsymbol{M_{ij}}\cdot\dot{\boldsymbol{U}}_i + \boldsymbol{A_{ij}}\cdot\boldsymbol{U}_i = \boldsymbol{b_i(U)} \qquad (11)$$

where,
$M_{ij} = (\Phi_j, \Phi_i)$ is the mass matrix
$A_{ij} = (\nabla\Phi_j, \nabla\Phi_i)$ is the stiffness matrix
$b_i(U) = (f(U_i), \Phi_i)$ is the non-linear load vector

The time dependent part of Equation (11) is discretized further into system of non-linear algebraic equations using the highly stable backward-difference formula. Thus, Equation (12) becomes:

$$(M_{ij} + k \cdot A_{ij}) \cdot (U_n)_i = M_{ij} \cdot (U_{n-1})_i + k \cdot b_i(U_n) \quad (12)$$

where, k is the time step size and n is time step level.

To solve the sets of non-linear algebraic equations given by Equation (12), it is necessary to use the Newton's-Raphson iterative scheme which involves solving a linearized form of the equation iteratively using an initial guess and Jacobian matrix as expressed in Equation (13). The numerical implementation was carried out in MATLAB. A mesh with parameter value, $h_{\max} = 0.0125$, that was used for the analysis (as shown in Figure 1 (b)). A time step of $k = 0.01$ was used for a normalized total time of 10, which is equivalent to 833.33 minutes of phase separation in zirconia.

$$J_{ij} = \frac{\partial F_i}{\partial (U_n)_j} = \left[M_{ij} + k \cdot A_{ij} \right] - 0 - k \frac{\partial b_i(U_n)}{\partial (U_n)_j} \quad (13)$$

where,

$$F_i = (M_{ij} + k \cdot A_{ij}) \cdot (U_n)_i - M_{ij} \cdot (U_{n-1})_i - k \cdot b_i(U_n) = 0 \quad (14)$$

Fourier Spectral Methods

Recently, spectral methods are widely used to solve nonlinear PDEs. While other schemes such as FDM and FEM uses local representation of the PDEs to arrive at numerical solution in time domain, spectral methods uses global representation discretized in Fourier space (having higher order) to arrive at numerical solution in frequency scale. Consequently, the spectral methods are faster, less intensive and exhibit a higher order of accuracy especially when applied to highly non-linear PDEs (Hussaini *et al*., 1983). However, spectral methods are reported to have difficulties with boundary conditions, sometimes resulting in an ill-posed problem with lots numerical instabilities (Shu and Wong, 1996). Currently, the method is only suitable for problems with periodic boundary conditions applied on regular geometries.

In the present study, the Allen-Cahn equation is discretized with Galerkin spectral method in which the PDE is expressed as a finite expansion of some sets of global basis function. Thus, the PDE is first transformed into the Fourier space by taking the Fast Fourier Transform (FFT) of both sides of equation as expressed in Equation (5).

$$\frac{\partial \hat{\eta}_{1k}}{\partial \bar{t}} = \hat{\eta}_{1k} - \left(\eta_1^3\right)_k + \varepsilon \cdot \bar{\nabla}^2 \hat{\eta}_{1k} = \hat{\eta}_{1k} - \left(\eta_1^3\right)_k + \varepsilon \cdot \left((ik_x)^2 \cdot \hat{\eta}_{1k} + (ik_y)^2 \cdot \hat{\eta}_{1y} \right) \quad (15)$$

By applying the backward difference formula to the time derivative, Equation (16) reduces to:

$$\frac{\hat{\eta}_{1k}{}^n - \hat{\eta}_{1k}{}^{n-1}}{h} = \hat{\eta}_{1k}{}^{n-1} - (\eta_1^3)_k{}^{n-1} + \varepsilon \cdot ((ik_x)^2 \eta_{1k}{}^n + (ik_y)^2 \eta_{1k}{}^n) \quad (16)$$

After re-arranging, the final form of discrete equation can be represented as:

$$\hat{\eta}_{1k}{}^n = \frac{\hat{\eta}_{1k}{}^{n-1} \cdot \left(\frac{1}{h} + 1 \right) - (\eta_1^{n-1})^3}{-\varepsilon \cdot \left((ik_x)^2 + (ik_y)^2 - \frac{1}{h\varepsilon} \right)} \quad (17)$$

From Equation (17), the dependent variable is solved in Fourier space, after which the solution is in converted back into time space. The numerical implementation was also carried out in MATLAB with a grid parameter of $h = 0.0125$ and time step of $k = 0.01$ was used for the computation. Similarly, the PDE was solved in the domain for total normalized time of 10.

RESULTS AND DISCUSSION

Numerical results obtained with FEM

Figure 3 shows the numerical value of the order parameter indicating the various coexisting phases existing at last time step (i.e. $\bar{t} = 10$) of computation. It can be seen from the figure that, the interface thickness increases with an increase in the normalization parameter, ε. This is because of the strong correlation between interfacial (or gradient) energy and interface thickness (Chen, 2002). The normalization parameter is a direct function of the gradient energy coefficient or the interfacial energy. Consequently, it is expected that more energy is required for the evolution or transformation involving thicker material interfaces (as depicted by Figure 3). Figure 3(a) shows the evolution of phases for realistic (zirconia) normalization parameter of $\varepsilon = 5 \times 10^{-5}$ determined from the works (Abubakar *et al*., 2015). Figure 3(b) and (c) shows that the phase evolution proceeds with thicker interfaces and higher transformation energy when higher numerical value of the normalization parameter is used. Interestingly, Figure 3 (c) shows reordering of phases due to high variation of interfacial energy during the transformation as previously found (Danilov and Nestler, 2005), (Zaeem, 2010).

Therefore, it can be said that the Allen-Cahn equation has adequately captured the important role of energy state of interfaces on phase transformation in materials. As we reduced the normalization parameter (and interfacial energy) to very low value, we observed divergence of numerical solution of the non-linear PDE. This is because the interfacial energy is too small to create an interface that will drive the phase transformation as previously found (Chen, 2002; Moelans *et al*., 2008).

Figure 3(d) shows contour plots of order parameter and coexisting phases as computed by the commercial finite element package, COMSOL Multiphysics. The solution compares well with that of Figure 3(a) which was obtained with the FE code developed in MATLAB. The power of the Allen-Cahn PDEs in separating phases within a material microstructure can clearly be seen. Phase separation phenomenon is a very interesting process and modeling it has enabled engineers to correlate the relationship between the structure and properties/performance of materials more effectively.

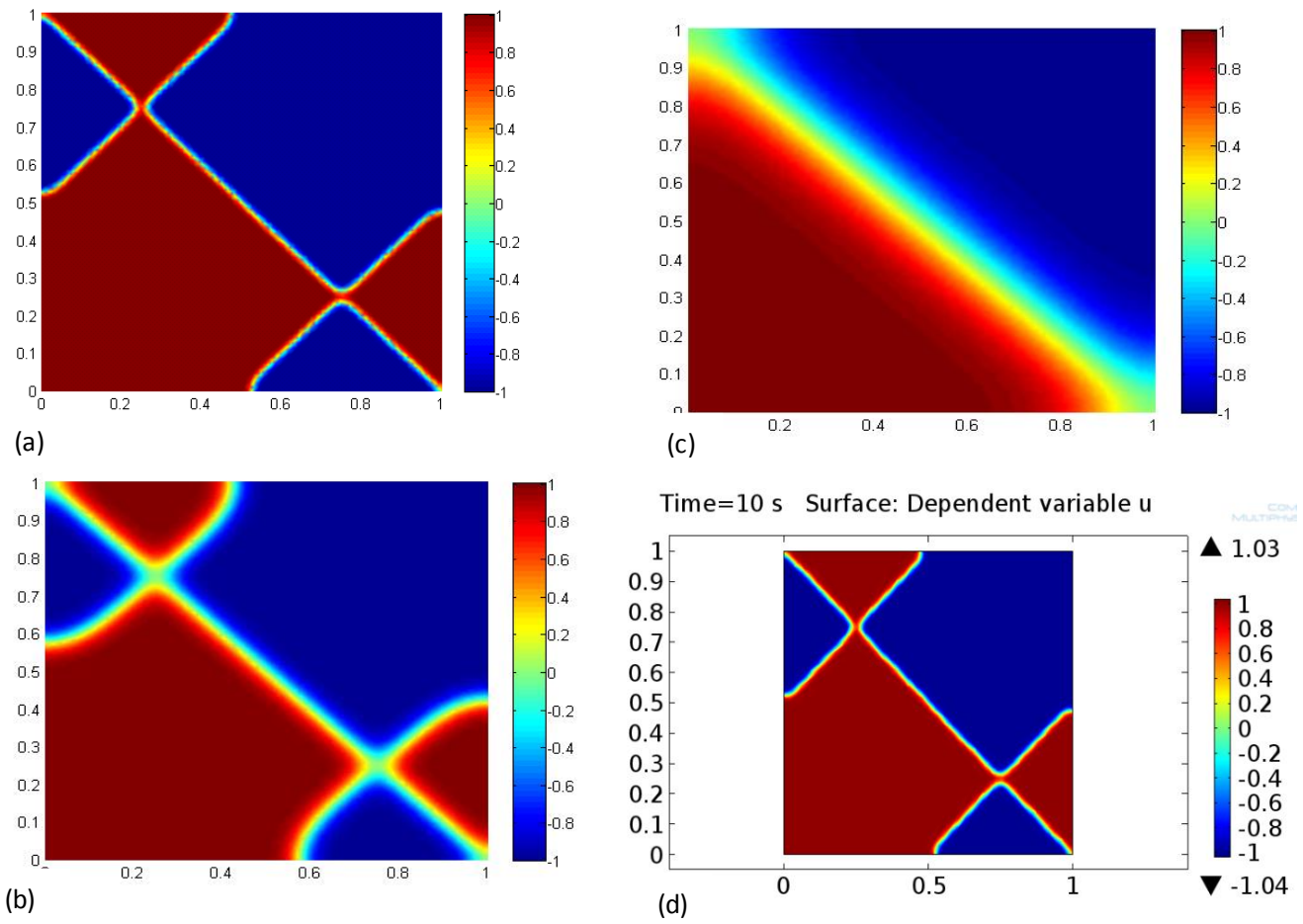

Figure 3: Allen-Cahn order parameter after $\bar{t} = 10$: (a) $\epsilon = 5 \times 10^{-5}$, (b) $\epsilon = 5 \times 10^{-3}$ (c) $\epsilon = 5 \times 10^{-1}$ (d) $\epsilon = 5 \times 10^{-5}$(from COMSOL)

Numerical results obtained with FSM

Figure 5 shows the numerical solution of the PDE when the FSM is used for the computation. It is important to mention that the figure shows the plot of the solution in 3D for grid size of h = 0.0125 and time step of k=0.01. It can be clearly seen that the FSM and FEM solutions look alike with very minor deviation of results at the interfaces.

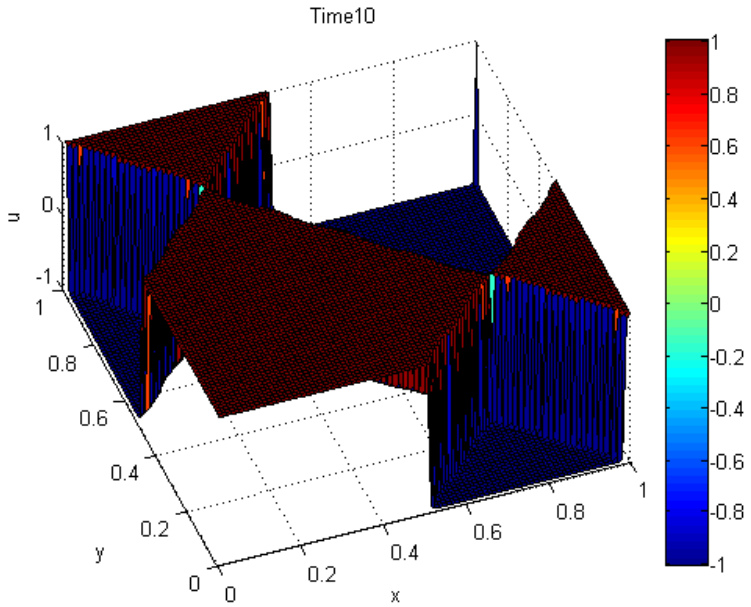

Figure 5: Allen-Cahn order parameter after $\bar{t} = 10$ using the FSM code

Comparison of numerical accuracy and efficiency of the numerical schemes

For the purpose of evaluating the numerical accuracy of solution obtained with the two schemes, the variation of order parameter with grid size and time step is tracked at two points, A and B (as shown in Figure 6). Figure 6 (a) and (b) shows the variation of the order parameter with mesh size at the points A and B respectively. It can be seen that, the FSM scheme converges to the actual solution with less than 20 nodes. While, the FEM scheme requires denser mesh having about 50-175 nodes (depending on location) for the solution to converge. This is because the FSM scheme was developed based on polynomials of higher order, O (NlogN), as compared to FEM, O (N2). Thus, the FSM scheme is more effective in modeling phase transformation problems.

In a similar fashion, Figure 6 (c) and (d) shows how the time step size affects the solution obtained with both schemes. It can be seen that, the FSM is severely affected by variation in time step than the FEM even though Backward-Euler finite difference method was used to discretize both schemes. This happens because the stability bound of the FSM scheme used here is highly restricted to the time step size. Thus, we found that after time step of 1, the FSM scheme becomes highly unstable and leads to very inaccurate results as expected.

Figure 7 (a) and (b) shows that the FSM scheme is less computationally intensive than the FEM scheme. Computation using the FSM scheme completes within shorter time (about 10 seconds) as compared to that of the FEM scheme (i.e. about 230 seconds). This is because the FEM scheme requires the repetitive task of assembling the stiffness and mass matrices. Additionally, the Newton's method used for the computation involves much iteration that consumes longer time. But with the FSM scheme, the non-linearity is treated explicitly. This implies that the computational domain is discretized in the Fourier space with global basis functions of higher order. Consequently, the FSM code exhibits higher numerical efficiency. This is very advantageous when modeling highly non-linear process like phase transformation.

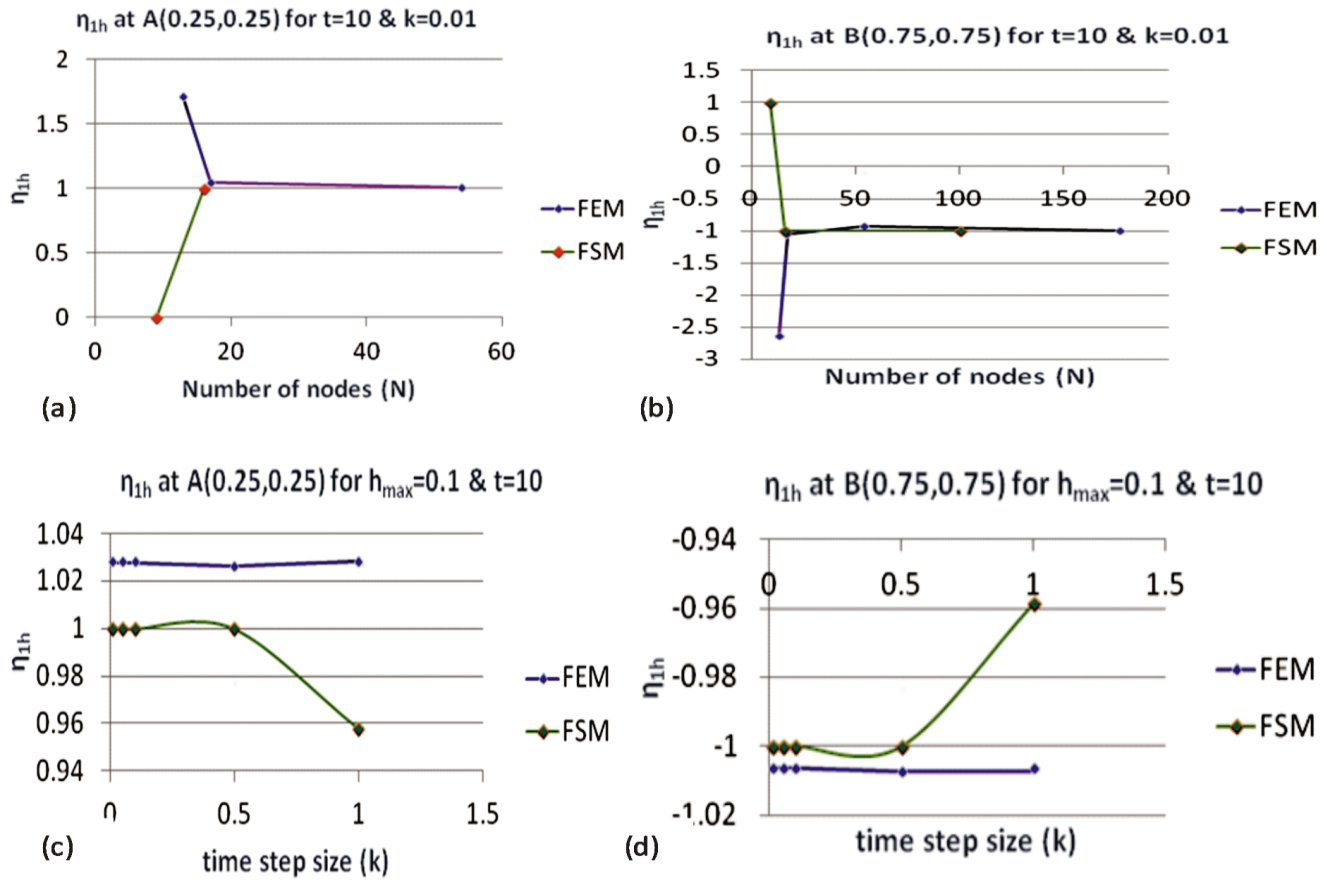

Figure 6: Variation of the order parameter with: (a) mesh size at A, (b) mesh size at B, (c) time step at A, and (d) time step B

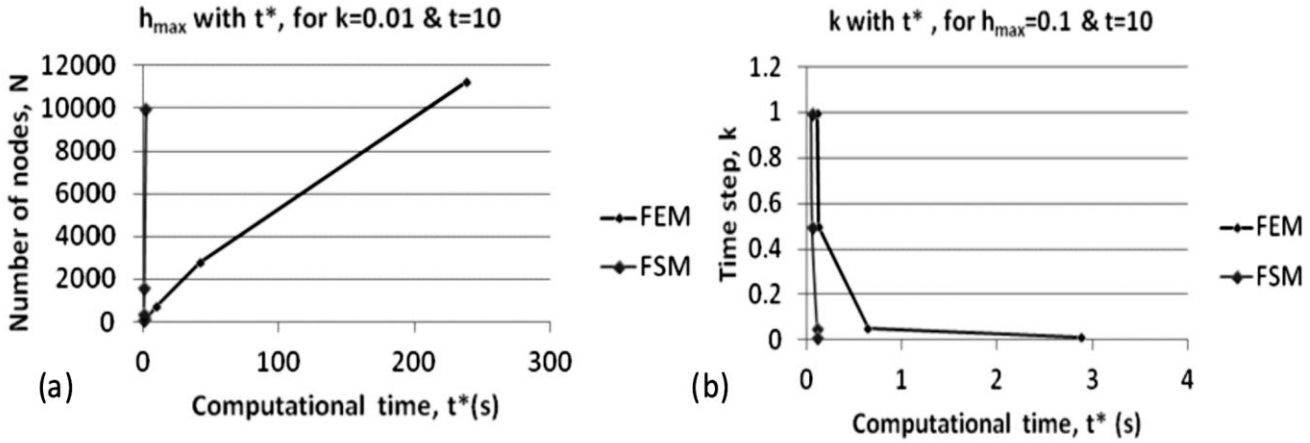

Figure 7: Variation of computation time with: (a) mesh size and (b) time step

CONCLUSIONS

Non-linear phase transformation equation based on Allen-Cahn theory was analyzed numerically based on the Galerkin's Finite Element Method (FEM) and Galerkin's Fourier Spectral Method (FSM). Numerical implementation was carried out in the commercial package, MATLAB. The results show that the FSM scheme is very effective tool for the numerical modeling of material phase transformations problems due to its high computational efficiency and accuracy. The FEM scheme consumes higher computational resources due to the need for repetitive assembly of several matrices. Furthermore, due to discretization with polynomials of relatively lower order, the FEM scheme requires a denser mesh for successful convergence of numerical results. This further reduces the computational efficiency of the FEM scheme. However, the FSM scheme has drawbacks that render its applicability and efficiency when applied to problems of certain kind. The scheme becomes highly unstable and inaccurate when applied to problems that require larger time step and intricate computational domains. Therefore, more research needs to be carried out in developing more stable FSM schemes in future works.

ACKNOWLEDGEMENT

The authors acknowledge the support given by Bayero University Kano in conducting the research work.

REFERENCES

Abubakar, A. A., Akhtar, S. S., Arif, A. F. M., 2015. Phase field modeling of V2O5 hot corrosion kinetics in thermal barrier coatings. Comput. Mater. Sci. 99. https://doi.org/10.1016/j.commatsci.2014.12.004.

Allen, S. M., Cahn, J.W., 1979. A microscopic theory for antiphase boundary motion and its application to antiphase domain coarsening. Acta Metall. 27, 1085–1095.

Cahn, J. W., Hilliard, J. E., 1958. Free Energy of a Nonuniform System. I. Interfacial Free Energy. J. Chem. Phys. 28.

Chen, L.-Q., 2002. Phase-field models for microstructure evolution. Annu. Rev. Mater. Res. 32, 113–140.

Danilov, D., Nestler, B., 2005. Phase-field simulations of solidification in binary and ternary systems using a finite element method. J. Cryst. Growth 275, e177–e182.

Furihata, D., Matsuo, T., 2003. A stable, convergent, conservative and linear finite difference scheme for the Cahn-Hilliard equation. Jpn. J. Ind. Appl. Math. 20, 65.

Hussaini, M. Y., Streett, C. L., Zang, T. A., 1983. Spectral methods for partial differential equations.

Kobayashi, R., 1993. Modeling and numerical simulations of dendritic crystal growth. Phys. D Nonlinear Phenom. 63, 410–423. https://doi.org/http://dx.doi.org/10.1016/0167-2789(93)90120-P

Lee, H. G., Shin, J., Lee, J.-Y., 2017. A Second-Order Operator Splitting Fourier Spectral Method for Models of Epitaxial Thin Film Growth. J. Sci. Comput. 71, 1303–1318. https://doi.org/10.1007/s10915-016-0340-4

Li, D., Qiao, Z., 2017. On Second Order Semi-implicit Fourier Spectral Methods for 2D Cahn–Hilliard Equations. J. Sci. Comput. 70, 301–341. https://doi.org/10.1007/s10915-016-0251-4

Moelans, N., 2006. Phase-field simulations of grain growth in materials.

Moelans, N., Blanpain, B., Wollants, P., 2008. An introduction to phase-field modeling of microstructure evolution. Calphad 32, 268–294. https://doi.org/http://dx.doi.org/10.1016/j.calphad.2007.11.003.

Raabe, D., 1998. Modeling and Simulation in Materials Science, in: Computational Materials Science. Wiley-VCH Verlag GmbH and Co. KGaA, pp. 13–28. https://doi.org/10.1002/3527601945.ch2.

Shu, C. W., Wong, P. S., 1996. A numerical study on the accuracy of fourier spectral methods applied to the nonlinear burgers equation, in: Proceedings of the Third International

Conference on Spectral and High Order Methods, AV Ilin and LR Scott, Editors, Houston Journal of Mathematics. pp. 131–138.

Vidyasagar, A., Tan, W. L., Kochmann, D. M., 2017. Predicting the effective response of bulk polycrystalline ferroelectric ceramics via improved spectral phase field methods. J. Mech. Phys. Solids 106, 133–151. https://doi.org/https://doi.org/10.1016/j.jmps.2017.05.017.

Vollmayr-Lee, B. P., Rutenberg, A.D., 2003. Fast and accurate coarsening simulation with an unconditionally stable time step. Phys. Rev. E 68, 66703.

Voyiadjis, G. Z., Mozaffari, N., 2013. Nonlocal damage model using the phase field method: theory and applications. Int. J. Solids Struct. 50, 3136–3151.

Wen, Y. H., Chen, L.-Q., Hawk, J. A., 2012. Phase-field modeling of corrosion kinetics under dual-oxidants. Model. Simul. Mater. Sci. Eng. 20, 35013.

Zaeem, M. A., 2010. Finite element method for conserved phase field models: Solid state phase transformations. Washington State University.